

氏 名	ぬま くら ひろし 沼 倉 宏
授 与 学 位	工 学 博 士
学位授与年月日	昭和 61 年 3 月 25 日
学位授与の根拠法規	学位規則第 5 条第 1 項
研究科, 専攻の名称	東北大学大学院工学研究科 (博士課程) 原子核工学専攻
学 位 論 文 題 目	Hydride precipitation and lattice defects in titanium and zirconium (チタンおよびジルコニウム中の水素化物析出と格子欠陥 に関する研究)
指 導 教 官	東北大学教授 平林 真
論 文 審 査 委 員	東北大学教授 平林 真      東北大学教授 小岩 昌宏 東北大学教授 諸住正太郎      東北大学教授 鈴木 秀次

## 論 文 内 容 要 旨

### CHAPTER 1 GENERAL INTRODUCTION

Titanium and zirconium, being group IV transition metals, are very important materials in technology. In the application of these metals as structural materials, there exist two basic metallurgical problems: (1) hydrogen embrittlement, and (2) ductility of polycrystals.

The former is characteristic of the hydride-forming metals such as group IVa and group Va metals. These metals can absorb a considerable amount of hydrogen, whereas the solid solubility of hydrogen is generally not so large. When the hydrogen concentration exceeds the solubility limit, precipitation of hydride occurs and mechanical properties are deteriorated due to the brittle nature of the hydrides. In the present study, precipitation of hydride in titanium and zirconium has been investigated systematically; the solubility of hydrogen and deuterium, the crystal structure of hydrides, their morphology and mechanism of precipitation are studied by internal friction, electron, X-ray and neutron diffraction, and transmission

electron microscopy.

The second problem, the polycrystalline ductility, is relevant to the crystal structure of titanium and zirconium; the hexagonal close-packed (h. c. p.) structure. In the plastic deformation of h. c. p. polycrystals, the  $\langle \bar{1}\bar{1}23 \rangle$  slip is particularly important because the primary  $\langle 11\bar{2}0 \rangle$  slip cannot accommodate any dimensional change along the [0001] direction. The  $\langle \bar{1}\bar{1}23 \rangle$  slip must be an active deformation mode in titanium and zirconium since these metals actually exhibit good ductility. In order to elucidate the mechanism of  $\langle \bar{1}\bar{1}23 \rangle$  slip, properties of  $1/3\langle \bar{1}\bar{1}23 \rangle$  dislocations are investigated from an atomistic point of view, by computer simulation of the core structure in model h. c. p. crystals, and by electron microscopic observations of the dislocations in deformed titanium.

## CHAPTER 2 HYDRIDE PRECIPITATION IN TITANIUM AND ZIRCONIUM

### 2.1. Internal friction in Ti-H, Ti-D, Zr-D alloys

The terminal solubilities of hydrogen and deuterium in titanium and zirconium have been determined from the hydride precipitation and dissolution peaks in internal friction. The solubility of hydrogen and that of deuterium are approximately the same in these metals. The large thermal hysteresis between the solvus temperature on heating and that on cooling, which amounts to 50 K, can be accounted for in terms of the misfit strain energy associated with the precipitation.

### 2.2. Diffraction study on the formation of $\gamma$ titanium hydride

According to the previously reported Ti-H phase diagram, the  $\delta$  hydride phase, which has a face-centred cubic structure, is to precipitate in the  $\alpha$  phase matrix on crossing the solvus temperature downwards. However, the present investigation has demonstrated that the hydride formed in titanium specimens containing 1 - 3 at.% H or D is a new hydride phase, having a face-centred tetragonal structure with  $c/a=1.09$ . The crystal structure of the hydride has been studied by electron diffraction, X-ray and neutron powder diffraction using Rietveld analysis. This hydride has been found to be very similar to the metastable  $\gamma$  zirconium hydride in the Zr-H system, and thus the new hydride phase has been named  $\gamma$  titanium hydride. This structure can be described by the space group  $P4_2/n$  (tetragonal), and the co-ordinates of the atoms in the unit cell are as follows:

4 Ti in 4 c:  $1/4, 1/4, 1/4$ ;  $3/4, 3/4, 1/4$ ;  $1/4, 3/4, 3/4$ ;  $3/4, 1/4, 3/4$ .

2 H in 2 b:  $0, 0, 1/2$ ;  $1/2, 1/2, 0$ .

2 H in 2 a:  $0, 0, 0$ ;  $1/2, 1/2, 1/2$ .

According to this structure model, this hydride corresponds to the composition TiH.

### 2.3. Transmission electron microscopy on hydride precipitation in titanium

The morphology, the habit plane of the  $\gamma$  hydride, and the orientation relationship between the hydride and the  $\alpha$  titanium matrix are studied by electron microscopic observations. It has been found that there are two types of precipitation mode: type I and type II. The precipitation is accompanied by misfit stresses due to the larger specific volume of the hydride than that of the matrix phase. The stresses are accommodated mainly by elastic distortion for the type I precipitates, while for the type II they are relaxed plastically, i. e., by dislocation generation. Possible atomic mechanisms of the precipitation are discussed in the light of these observations.

## CHAPTER 3 CORE STRUCTURE AND GLIDE BEHAVIOUR OF $1/3\langle\bar{1}\bar{1}23\rangle$ DISLOCATIONS IN TITANIUM AND ZIRCONIUM

### 3.1. Electron microscopic observation of $1/3\langle\bar{1}\bar{1}23\rangle$ dislocations in titanium

In polycrystalline titanium specimens deformed to 3~4 % strain at room temperature,  $1/3\langle\bar{1}\bar{1}23\rangle$  dislocations are frequently observed in addition to the  $1/3\langle\bar{1}\bar{1}20\rangle$  dislocations. The  $1/3\langle\bar{1}\bar{1}23\rangle$  dislocations have been shown to glide exclusively on  $\{10\bar{1}1\}$  planes. One interesting feature of these dislocations is that they are aligned nearly parallel to the  $\langle\bar{1}210\rangle$  direction, i. e., the close-packed direction, indicating that the dislocation in this orientation are less mobile than the others.

### 3.2. Computer simulation of core structure of $1/3\langle\bar{1}\bar{1}23\rangle\{10\bar{1}1\}$ dislocations in a model h. c. p. crystal

The intrinsic properties of  $1/3\langle\bar{1}\bar{1}23\rangle$  dislocations, viz., the core structure and the mechanism of glide motion, are studied by computer simulation using a model crystal constructed with a truncated Lennard-Jones interatomic potential.

Simulation has been performed on four different  $1/3\langle\bar{1}\bar{1}23\rangle$  dislocations. Three of those

are non-screw  $1/3[\bar{1}\bar{1}2\bar{3}]$  dislocations on  $(10\bar{1}1)$ , viz., (1) a mixed dislocation of  $\phi=75^\circ$ , the dislocation line direction being parallel to  $[\bar{1}2\bar{1}0]$  direction, (2) an 'edge' dislocation of  $\phi=91^\circ$ , (3) a mixed dislocation of  $\phi=150^\circ$  (where  $\phi$  is the angle between the Burgers vector and the dislocation line direction), and the fourth is the screw dislocation ( $\phi=0^\circ$ ). Among those the first one is of particular interest since the  $1/3\langle\bar{1}\bar{1}2\bar{3}\rangle$  dislocations observed experimentally in titanium and its alloys are mostly of this type.

In all the four cases studied, the relaxed core configuration shows planar spread on the  $(10\bar{1}1)$  plane associated with stacking faults. On the  $\{10\bar{1}1\}$  plane of h. c. p. crystals, two stacking faults,  $F_1$  and  $F_2$ , have been predicted to exist by atomistic calculations. Therefore, the  $1/3\langle\bar{1}\bar{1}2\bar{3}\rangle$  dislocations are expected to be dissociated into three partial dislocations,  $b_3, b_2$  and  $b_1$ , with the faults  $F_2$  and  $F_1$  bounded by these partials. The core structures of the 'edge', the  $150^\circ$  mixed- and the screw dislocations are almost in accordance with this expectation; the core configuration and the splitting scheme of the Burgers vector are illustrated in Figs. 1a and 2a, respectively. On the other hand, the relaxed core structure of the  $75^\circ$  mixed dislocation has been found to be different from the three dislocations; the dislocation is dissociated into two partials, and only the fault  $F_1$ , which has the lower stacking fault energy, exists, as depicted in Figs. 1b and 2b.

When shear stresses are applied, the extended dislocations comprising the three partials glide on  $(10\bar{1}1)$  easily under small stresses less than  $0.01G$  without any marked change of the core structure. In contrast to this, the net motion of the  $75^\circ$  dislocation occurs at stresses above  $0.03G$ ; the mixed partial has been dissociated further into the two elementary partials prior to the glide motion, and the total dislocation glides with a configuration of the three partials, in the same way as the other three orientations.

An expectation from the present simulation study is that the shear stress required for the motion of the  $1/3\langle\bar{1}\bar{1}2\bar{3}\rangle$  dislocation on the  $\{10\bar{1}1\}$  plane is the largest when the dislocation line is parallel to  $\langle\bar{1}2\bar{1}0\rangle$  (i. e., the  $75^\circ$  orientation), and consequently the mobility is the lowest. This feature is in excellent agreement with the experimental observations of the dislocation configuration in deformed titanium. It is conceivable, therefore, that the glide mechanism of  $1/3\langle\bar{1}\bar{1}2\bar{3}\rangle$  dislocations in titanium, zirconium and their alloys is similar to that suggested by the present simulation. The glide occurs on  $\{10\bar{1}1\}$  by motion of the three partial dislocations,  $b_3, b_2$  and  $b_1$ . In that case, in polycrystalline materials in which the  $\langle\bar{1}\bar{1}2\bar{3}\rangle$  slip is necessary, the macroscopic deformation rate would be controlled by the

motion of the  $75^\circ$  segments of the  $1/3\langle\bar{1}1\bar{2}3\rangle$  dislocations; this process itself is considered to occur by thermally activated transformation of the core structure from the stable two partial configuration into the glissile three partial configuration.

#### CHAPTER 4 SUMMARY AND SUGGESTIONS FOR FUTURE WORK

In this chapter, the principal results obtained by the present study are summarized, and some suggestions for further investigations are described.



Fig. 1. Possible core extension of a  $1/3\langle\bar{1}1\bar{2}3\rangle$  dislocation on  $\{10\bar{1}1\}$ . (a) Dissociation into three partial dislocations  $b_3$ ,  $b_2$  and  $b_1$  with the two enclosed stacking faults  $F_2$  and  $F_1$ . (b) Dissociation into two partial dislocations  $(b_3+b_2)$  and  $b_1$  with the fault  $F_1$ .

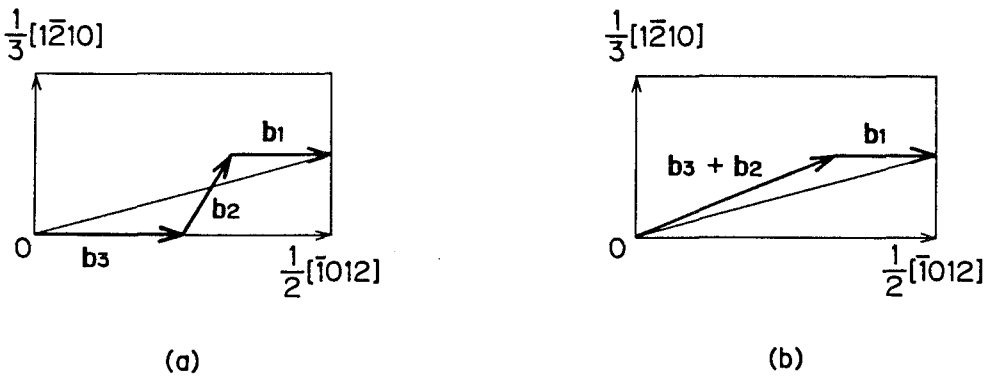


Fig. 2. Splitting of the Burgers vector  $b = 1/3[\bar{1}1\bar{2}3]$  on  $(10\bar{1}1)$ . (a)  $b \rightarrow b_3 + b_2 + b_1$  with  $F_2$  and  $F_1$ ; (b)  $b \rightarrow (b_3+b_2) + b_1$  with  $F_1$ , where  $b_3 = 1/4[\bar{1}012]$ ,  $b_2 = 1/12[1432]$  and  $b_1 = 1/6[\bar{1}012]$ .

## 審査結果の要旨

チタン (Ti) およびジルコニウム (Zr) は優れた化学的および機械的性質を有する金属であり、原子力工業をはじめとする工業分野で広く使用されている。これらの金属を実用材料として使用する上での種々の問題点の中で、基礎的視点からの解明が望まれているものとして水素脆性および多結晶材料の変形特性が挙げられる。本論文はこれら2つの点に関連して行った、水素化物の構造と析出および転位の芯構造に関する研究結果をまとめたものである。

第1章は序論である。

第2章ではTiおよびZrの水素化物について、種々の実験方法による研究の結果をのべており、以下の様に要約できる。

- (1) 内部摩擦測定により水素および重水素の固溶度を決定し、水素化物の溶解・析出のヒステリシスについて定量的な検討を行った。
- (2) Ti-H系には $\delta$ 相と呼ばれる面心立方構造の水素化物相 $TiH_{2-x}$ があることが知られている。しかし、少量の水素を含むTiを冷却する際に析出する水素化物は、従来の状態から予測される $\delta$ 相ではなく、面心正方構造 ( $c/a=1.09$ ,  $r$ 相) であることを明らかにし、X線回折、中性子回折によりその構造を決定した。
- (3) 上述の $r$ 相の析出挙動を透過電子顕微鏡観察により調べ、2種の析出形態があることを示し、その晶癖を決定した。

第3章では最密六方晶構造を有するTi, Zrの多結晶体の変形において、重要な役割を担う $1/3 \langle \bar{1} \bar{1} 2 \bar{3} \rangle$ 転位に関する研究結果をのべている。計算機シミュレーションにより、この転位の芯構造を、とくに転位線の方位との関連に着目して調べ、転位線とバーガース・ベクトルが $75^\circ$ をなす混合転位は特殊な芯構造を有することを見出し、さらに応力を加えた場合の各種転位の運動状態における芯構造を調べた。その結果から、 $\{10\bar{1}1\}$ 面上の $1/3 \langle \bar{1} \bar{1} 2 \bar{3} \rangle$ 転位を動かすに要する応力は、 $75^\circ$ 方位の転位に対して最大であり、したがってその易動度は最小であると予測した。著者自身および他の研究者による転位線の分布配列状態の電子顕微鏡観察の結果は、この予測とよい一致を示している。

第4章は結論である。

以上要するに本論文は、TiおよびZrについて、水素化物の構造、析出・溶解過程、析出形態について詳細に研究を行い、新しい水素化物相の存在を見出すとともに、六方晶金属中の転位芯構造を計算機シミュレーションにより調べいくつかの重要な知見を加えたものであって、原子核工学および材料工学の発展に寄与するところが少なくない。

よって、本論文は工学博士の学位論文として合格と認める。